Structural Eng./Earthquake Eng., JSCE, Vol. 16, No. 1, 21s—30s, 1999 April
(J. Struct. Mech. Earthquake Eng., JSCE, No. 619/ I —47)

FORMULATION OF IDENTIFYING MATERIAL PROPERTY DISTRIBUTION BASED ON EQUIVALENT INCLUSION METHOD

Muneo HORI[1], Toshihiro KAMEDA[2]and Naoyuki HOSOKAWA[3]

[1]Earthquake Research Institute, University of Tokyo (Yayoi, Bunkyo, Tokyo 113-0032, Japan)
[2]Institute of Engineering Mechanics, University of Tsukuba
(Tenoudai 1-1-1, Tsukuba, Ibaraki 305-8573, Japan)
[3]Tokyo Gas Company (Kaigan 1-5-20, Minato, Tokyo 105-8527, Japan)

A new formulation of an inverse problem of identifying a material property distribution is proposed. The formulation is based on the equivalent inclusion method which solves a heterogeneous body problem using a homogeneous body. Two linear inverse problems are obtained, and, due to the linearity, the limitation of identifying the distribution is clearly seen. Two illustrative problems are studied. For the first problem, quantities which can be identified and those which cannot be determined are clarified. For the second problem, the stress distribution is obtained by measuring strain distribution, even though the constitutive relation is not known.

Key Words *: inversion, inverse problem formulation, equivalent inclusion method*

1. INTRODUCTION

It is a challenging problem to identify a material property distribution in a heterogeneous body using data of limited quality and quantity regarding to its responses. This is an inverse problem, and a huge amount of researches have been carried out in various fields of engineering and science; see Tanaka and Bui[1)] and Bui[2)] for a concise list of related references; see also Kubo[3)]. In particular, the identification of the material property distribution from data measured on the boundary is practically important. In civil engineering, typical examples are the identification of the permeability distribution, the velocity structure, and the damaged area[4),5)]; see also related references[6),7),8)]. While the difficulty in solving these inverse problems is pointed out on a mathematical point of view, it is not fully understood how much information can be obtained from the measured data. Such information is required in order to increase the available data by further measurement, and to identify the unknown properties more accurately even though the full identification is not possible.

In general, the formulation[1] of identifying a material property distribution is straightforward. As responses of a heterogeneous body are given as a solution of a boundary value problem, the identification is formulated as an optimization problem, i.e., the material property distribution is determined as the one that minimizes a suitable error, which is defined as the difference of the responses computed by assuming a certain distribution of material property from the corresponding data that were actually measured. In this formulation, however, it is not easy to see the accuracy of the identification, since the dependence of the responses on the material property distribution is complicated. Furthermore, the difference between the computed responses and the measured data does not yield a sensitive measure to tell the accuracy; a large error in predicting the material property distribution far from the measured point may result in a small difference.

In this paper, we propose a new formulation of identifying material property distribution, based on the *equivalent inclusion method*[2] such that the limitation of the identification is clearly seen. The equivalent inclusion method replaces a heterogeneous body with a homogeneous body containing fictitiously introduced field variables, and solves the boundary value problem for the heterogeneous body using the solution of the homogeneous body problem. According to this method, a set of two inverse problems are formulated; the fictitious field variables in the homogeneous body are first identified from the boundary data, and then the material property distribution is determined from the identified field variables. These two inverse problems are linear to the unknown field variables and the unknown material property distribution, respec-

[1] In this paper, the formulation means just to pose a mathematical problem. Solving the posed problem is called the analysis, even though we need to formulate some equations for the analysis. The formulation and the analysis are thus distinguished.

[2] The equivalent inclusion method was originally proposed by Eshelby[10)] to solve an ellipsoidal inclusion problem in an elegant manner; see Nemat-Nasser and Hori[11)] for related references.

tively. Due to the linearity, it becomes transparent to distinguish quantities which can be identified from given data from those which cannot be determined, and hence the limitation of the identification is clarified.

This paper is organized as follows: Section 2 presents the formulation of the inverse problems based on the equivalent inclusion method. Identifying an elasticity moduli distribution is considered as a simple example, though the formulation can be easily applied to other material properties, such as permeability, thermal conductivity, etc. Two illustrative problems are studied in Sections 3 and 4. The first problem is a typical identification problem to find a permeability distribution for a heterogeneous porous medium, The second problem[3] is the identification of unknown elasto-plastic constitutive relation. The formulation of the inverse problems based on the equivalent inclusion method is presented for the two examples, and the limitation of the identification is discussed through numerical simulation and theoretical analysis.

To simplify mathematical expressions, we use both index and symbolic notations in this paper; for instance, displacement is denoted by $\boldsymbol{u}$ or u_i. In the index notation, the summation convention is employed and the derivative with respect to an x_i coordinate is denoted by a comma followed by a suffix i. In the symbolic notation, $\cdot$, : and $\otimes$ stand for the first and second order contraction and the tensor product, respectively, and ∇ is the differentiation operator.

2. GENERAL FORMULATION OF INVERSE PROBLEM

As a simple example, we consider a linearly elastic[4] heterogeneous body, V. The distribution of the elastic moduli, a field of a fourth-order elasticity tensor $(\boldsymbol{C})$, is the target of the analysis.

We consider a case when both displacement and traction are measured on some part of the boundary, S, as $\boldsymbol{u} = \overline{\boldsymbol{u}}$ and $\boldsymbol{t} = \overline{\boldsymbol{t}}$; see **Fig. 1**. The displacement is fixed on $T = \partial V - S$. An inverse problem of identifying $\boldsymbol{C}$ is usually formulated as the minimization problem of the following functional:

$$J(\boldsymbol{C}') = \int_S |\boldsymbol{t}(\boldsymbol{x}; \boldsymbol{C}') - \overline{\boldsymbol{t}}(\boldsymbol{x})|^2 \, \mathrm{d}S_{\boldsymbol{x}}. \tag{1}$$

Here, $\boldsymbol{t}$ is traction on S when $\boldsymbol{C}'$ is assumed, and computed by solving the following problem:

$$\begin{cases} \left(C'_{ijkl}(\boldsymbol{x})(u_{k,l}(\boldsymbol{x}; \boldsymbol{C}'))\right)_{,i} = 0 & \text{in } V, \\ u_i(\boldsymbol{x}; \boldsymbol{C}') = \overline{u}_i(\boldsymbol{x}) & \text{on } S, \\ u_i(\boldsymbol{x}; \boldsymbol{C}') = 0 & \text{on } T. \end{cases} \tag{2}$$

The dependence of $\boldsymbol{t}$ on $\boldsymbol{C}'$ is complicated, as the solution $\boldsymbol{u}$ is not linear with respect to $\boldsymbol{C}'$.

[3] This inverse problem is also formulated in the same manner as the above two problems, regarding unknown plastic strain as unknown field variables.

[4] The small deformation and the quasi-static state are assumed, though the proposed formulation can be applied to a more general setting.

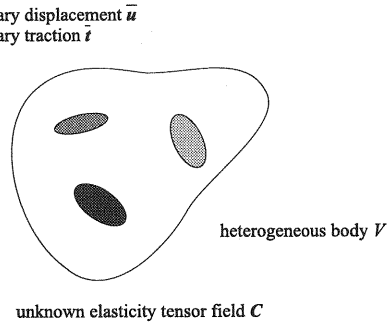

Fig. 1 Heterogeneous Body V

The equivalent inclusion method solves Eq. (Eq. (2)) using a homogeneous body, V^o, of the same configuration as V; see **Fig. 2**. Let the constant elasticity tensor of V^o be $\boldsymbol{C}^o$, and define a fictitious stress as $\boldsymbol{\sigma}^* = (\boldsymbol{C} - \boldsymbol{C}^o) : \boldsymbol{\epsilon}^e$, where $\boldsymbol{\epsilon}^e$ is a (yet-unknown) strain field of V. This $\boldsymbol{\sigma}^*$ is called *eigenstress*[5] or polarized stress. Then, Eq. (2) is rewritten as

$$\begin{cases} C^o_{ijkl} u_{k,li}(\boldsymbol{x}; \boldsymbol{\sigma}^*) + \sigma^*_{ij,i}(\boldsymbol{x}) = 0 & \text{in } V^o, \\ u_i(\boldsymbol{x}; \boldsymbol{\sigma}^*) = \overline{u}_i(\boldsymbol{x}) & \text{on } S, \\ u_i(\boldsymbol{x}; \boldsymbol{\sigma}^*) = 0 & \text{on } T. \end{cases} \tag{3}$$

While $\boldsymbol{\sigma}^*$ is yet unknown, we can solve Eq. (3) for any arbitrary $\boldsymbol{\sigma}^*$. The associated strain field is formally expressed as $\boldsymbol{\epsilon} = \boldsymbol{\epsilon}(\boldsymbol{x}; \boldsymbol{\sigma}^*)$, and $\boldsymbol{\sigma}^*$ must satisfy

$$(C_{ijkl}(\boldsymbol{x}) - C^o_{ijkl}) \epsilon_{kl}(\boldsymbol{x}; \boldsymbol{\sigma}^*) = \sigma^*_{ij}(\boldsymbol{x}). \tag{4}$$

This is an integral equation for $\boldsymbol{\sigma}^*$, called *consistency condition*. When $\boldsymbol{\sigma}^*$ is obtained by solving Eq. (4) the strain and stress fields produced by this $\boldsymbol{\sigma}^*$ coincide with those in V.

The equivalent inclusion method replaces (unknown) $\boldsymbol{C}$ with (unknown) $\boldsymbol{\sigma}^*$. Hence, we consider the following two inverse problems:

1. determine $\boldsymbol{\sigma}^*$ from Eq. (3) with the traction boundary data
2. identify $\boldsymbol{C}$ from Eq. (4) using $\boldsymbol{\sigma}^*$.

Now, we can formulate a linear inverse problem for $\boldsymbol{\sigma}^*$ instead of a minimizing problem similar to Eq. (1). We decompose $\boldsymbol{u} = \boldsymbol{u}^{(1)h} + \boldsymbol{u}^{(1)d}$, and pose the following boundary value problems in view of Eq. (3):

$$\begin{cases} C^o_{ijkl} u^{(1)h}_{k,li}(\boldsymbol{x}) = 0 & \text{in } V^o, \\ u^{(1)h}_i(\boldsymbol{x}) = \overline{u}_i(\boldsymbol{x}) & \text{on } S, \\ u^{(1)h}_i(\boldsymbol{x}) = 0 & \text{on } \partial V^o - S, \end{cases} \tag{5}$$

and

$$\begin{cases} C^o_{ijkl} u^{(1)d}_{k,li}(\boldsymbol{x}; \boldsymbol{\sigma}^*) + \sigma^*_{ij,i}(\boldsymbol{x}) = 0 & \text{in } V^o, \\ u^{(1)d}_i(\boldsymbol{x}; \boldsymbol{\sigma}^*) = 0 & \text{on } \partial V. \end{cases} \tag{6}$$

As is seen, $\boldsymbol{u}^{(1)d}$ is linear to $\boldsymbol{\sigma}^*$ in a sense of $\boldsymbol{u}^{(1)d}(\boldsymbol{\sigma}^* + \boldsymbol{\sigma}^{*\prime}) = \boldsymbol{u}^{(1)d}(\boldsymbol{\sigma}^*) + \boldsymbol{u}^{(1)d}(\boldsymbol{\sigma}^{*\prime})$. Using $\overline{\boldsymbol{t}}$ instead of $\overline{\boldsymbol{u}}$, we

[5] See also Sakurai[9] who seeks to identify inelastic strain of a body with unknown inelastic properties.

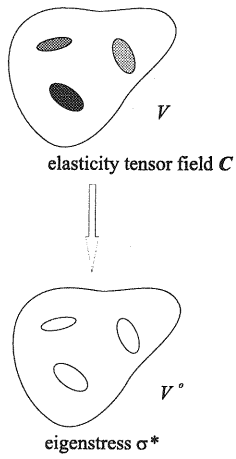

Fig. 2 Equivalent Inclusion Method

can derive another decomposition of $\boldsymbol{u} = \boldsymbol{u}^{(2)h} + \boldsymbol{u}^{(2)d}$ where $\boldsymbol{u}^{(2)d}$ is linear to $\boldsymbol{\sigma}^*$. Hence the first inverse problem of $\boldsymbol{\sigma}^*$ is formulated as

$$u_i^{(1)d}(\boldsymbol{x};\boldsymbol{\sigma}^*) - u_i^{(2)d}(\boldsymbol{x};\boldsymbol{\sigma}^*) = -u_i^{(1)h}(\boldsymbol{x}) + u_i^{(2)h}(\boldsymbol{x}). \tag{7}$$

Appendix presents an explicit expression of Eq. (7) using formal[6] Green functions of V^o.

Once $\boldsymbol{\sigma}^*$ is determined, we can formulate the second inverse problem of $\boldsymbol{C}$ as

$$C_{ijkl}(\boldsymbol{x})\epsilon_{kl}^{(1)}(\boldsymbol{x};\boldsymbol{\sigma}^*) = C_{ijkl}^o\epsilon_{kl}^{(1)}(\boldsymbol{x};\boldsymbol{\sigma}^*) + \sigma_{ij}^*(\boldsymbol{x}), \tag{8}$$

where $\boldsymbol{\epsilon}^{(1)}$ is the strain determined from $\boldsymbol{u}^{(1)h} + \boldsymbol{u}^{(1)d}$.

The strategy of formulating a pair of inverse problems can be applied to other material properties including non-linear cases, if suitable eigenfields and (non-linear) consistency conditions are introduced. The key is the replacement of the heterogeneity with the eigenfield such that a boundary value problem is posed for a suitable linear homogeneous body. We can expect two advantages[7] for the present formulation (in particular Eq. (7)), even though eigenstress is included as additional unknown field variables. The first is the linearity. Such linearity clarifies the validity as well as the limitation of analysis methods which are applied to solve these inverse problems. The second is that the data measured on the boundary are used to identify a second-order tensor field $\boldsymbol{\sigma}^*$, instead of a fourth-order tensor field $\boldsymbol{C}$.

[6] The solution presented in Appendix uses formal Green functions in a sense that they cannot be obtained unless numerically computed. In the subsequent sections, we apply the finite element method to solve the inverse problem, not the boundary element method.

[7] It should be emphasized that the proposed formulation does not change the nature of the problem, and does not identify quantities which cannot be determined by using other formulations.

3. EXAMPLE 1: PERMEABILITY IDENTIFICATION

Two illustrative problems of identifying a material property distribution are studied in the present and next sections. The main objective is to examine the advantages of the formulation of the inverse problems based on the equivalent inclusion method.

As the simplest example, we consider a two-dimensional heterogeneous porous medium[12] and seek to identify the distribution of permeability, $\boldsymbol{K}$, using pressure and flow data on some part of the boundary, $p = \overline{p}$ and $v = \overline{v}$ on S. Note that the displacement, strain and stress ($(\boldsymbol{u}, \boldsymbol{\epsilon}, \boldsymbol{\sigma})$ or $(u_i, \epsilon_{ij}, \sigma_{ij})$) and the elasticity tensor ($\boldsymbol{C}$ or C_{ijkl}) in the elastic body problem correspond to the pressure, pressure gradient and velocity ($(p, \boldsymbol{\psi}, \boldsymbol{\phi})$ or (p, ψ_i, ϕ_i)) and the permeability tensor ($\boldsymbol{K}$ or K_{ij}) in the porous medium problem.

First, we briefly summarize the equivalent inclusion method applied to the porous medium problem. When the pressure boundary data are used, the pressure satisfies

$$\begin{cases} (K_{ij}(\boldsymbol{x})p_{,j}(\boldsymbol{x}))_{,i} = 0 & \text{in } V, \\ p(\boldsymbol{x}) = \overline{p}(\boldsymbol{x}) & \text{on } S, \\ p(\boldsymbol{x}) = 0 & \text{on } \partial V - S. \end{cases} \tag{9}$$

The equivalent inclusion method introduces a homogeneous medium V^o with a constant permeability tensor, $\boldsymbol{K}^o$, and replaces the heterogeneity with the *eigenvelocity*, $\boldsymbol{\phi}^*$, such that Eq. (9) becomes

$$\begin{cases} K_{ij}^o p_{,ij}(\boldsymbol{x};\boldsymbol{\phi}^*) + \phi_{i,i}^*(\boldsymbol{x}) = 0 & \text{in } V^o, \\ p(\boldsymbol{x};\boldsymbol{\phi}^*) = \overline{p}(\boldsymbol{x}) & \text{on } S, \\ p(\boldsymbol{x};\boldsymbol{\phi}^*) = 0 & \text{on } \partial V^o - S. \end{cases} \tag{10}$$

The eigenvelocity satisfies its definition,

$$(K_{ij}(\boldsymbol{x}) - K_{ij}^o)\psi_j(\boldsymbol{x};\boldsymbol{\phi}^*) = \phi_i^*(\boldsymbol{x}). \tag{11}$$

We formulate a set of two inverse problems to identify unknown $\boldsymbol{K}$ from measured $\overline{p}$ and $\overline{v}$. Since Eq. (10) and Eq. (11) correspond to Eq. (3) and Eq. (11), we transform Eq. (7) and Eq. (8) to the inverse problem of $\boldsymbol{\phi}^*$ and $\boldsymbol{K}$. That is,

$$p^{(1)d}(\boldsymbol{x};\boldsymbol{\phi}^*) - p^{(2)d}(\boldsymbol{x};\boldsymbol{\phi}^*) = -p^{(1)h}(\boldsymbol{x}) + p^{(2)h}(\boldsymbol{x}), \tag{12}$$

$$K_{ij}(\boldsymbol{x})\psi_j^{(1)}(\boldsymbol{x};\phi^*) = K_{ij}^o\psi_j^{(1)}(\boldsymbol{x};\phi^*) + \phi_i^*(\boldsymbol{x}). \tag{13}$$

Here, $p^{(1)h}$ and $p^{(2)h}$ are due to $\overline{p}$ and $\overline{v}$ on S in the absence of $\boldsymbol{\phi}^*$, $p^{(1)d}$ and $p^{(2)d}$ are due to $\boldsymbol{\phi}^*$ for zero pressure and flux on S, and $\boldsymbol{\psi}^{(1)}$ is the pressure gradient associated with $p^{(1)h} + p^{(1)d}$; see Appendix A for a more explicit expression of Eq. (12). It should be emphasized that both $p^{(1)d}$ and $p^{(2)d}$ are linear to $\boldsymbol{\phi}^*$.

We consider a square V consisting of N^2 square regions with distinct anisotropic permeability tensors. The pressure and flow are measured at two horizontal edges of V, and the flux is fixed on two vertical edges. In the finite element analysis, we have $3N^2$ unknown permeability tensor components and $2N-1$

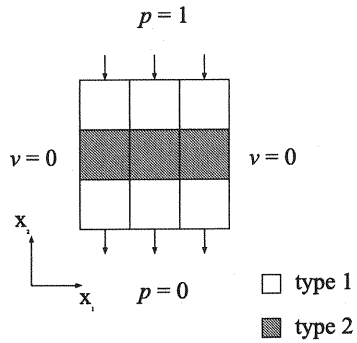

Fig. 3 Squere V with Heterogeneous Permeability Tensor

measured quantities; see Appendix B. If, say, $2N$ pressure data are used to solve a boundary value problem for p, then, $2N-1$ independent flux data are regarded as extra information. A homogeneous V^o is constructed with the same manner as V; see **Fig. 3**. Since In a discretized form, it is easier to use for the pressure gradient than the pressure, we obtain $p^{(1)d} - p^{(1)h})_{,i} = -(p^{(1)h} - p^{(2)h})_{,i}$ from Eq. (12), and express it in the following matrix form:

$$[\Delta g_{IP}]\,[\phi_P^*] = [\Delta\psi_I]\,, \tag{14}$$

where $[\Delta g_{IP}]$ is a $2N^2 \times 2N^2$ square matrix, and $[\phi_P^*]$ and $[\Delta\psi_I]$ are $2N^2$ vectors corresponding to $\boldsymbol{\phi}^*$ and $-(p^{(1)h} - p^{(2)h})_{,i}$; see Appendix B for the brief explanation of Eq. (14).

We consider a case of $N = 3$. The components of the permeable tensors used for V and V^o are summarized in **Table 1**. After solving a boundary value problem of V, an 18×18 matrix $[\Delta g_{IP}]$ and 18 vector $[\Delta\psi_P]$ in Eq. (14) are computed by solving the corresponding boundary value problems of V^o. The matrix $[\Delta g_{AP}]$ is not invertible and has the rank of 11, since the independent data are 7. Using eigenvectors of non-zero eigenvalues of $[\Delta g_{AP}]$, we can obtain a solution of Eq. (14) in the following form:

$$[\phi_P^*] = \left[\overline{\phi}_P^*\right] + [\phi_P^{**}]\,, \tag{15}$$

where $\left[\overline{\phi}_P^*\right]$ is a part of $[\phi_P^*]$ which can be determined from $[\Delta\psi_A]$, and $[\phi_P^{**}]$ is a part which cannot be determined as they satisfy $[\Delta g_{IP}]\left[\overline{\phi}_P^*\right] = [\Delta\psi_I]$ and $[\Delta g_{IP}]\,[\phi_P^{**}] = [0]$. **Figure 4** shows the distribution of $\left[\overline{\phi}_P^*\right]$. It also shows $[\phi_P^{**}]$ which is computed as the difference of the exact eigenvelocity and $\left[\overline{\phi}_P^*\right]$. While $[\phi_P^{**}]$ is not determined, $\left[\overline{\phi}_P^*\right]$ produces almost the same pressure gradient and velocity fields in the homogeneous body as those in the heterogeneous body; see **Fig. 5**.

In the numerical computation shown above, the reference permeability tensor $\boldsymbol{K}^o$ is chosen as the permeability tensors of elements of the top and bottom

Table 1 Permeable Tensors

	type 1	type 2	$\boldsymbol{K}^o$
K_{11}	−1.	−2.	−1.
K_{22}	−1.	−2.	−2.
K_{12}	0.	0.	0.

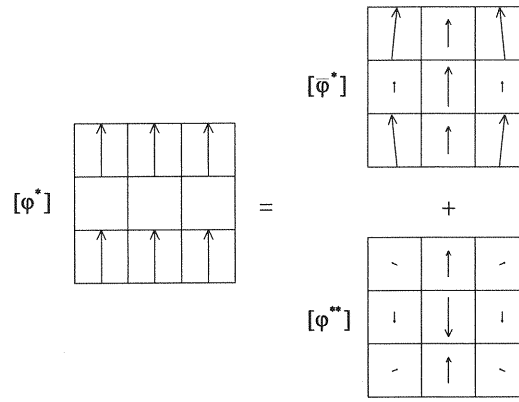

Fig. 4 Determined and Undetermined Eigenvelocity Components

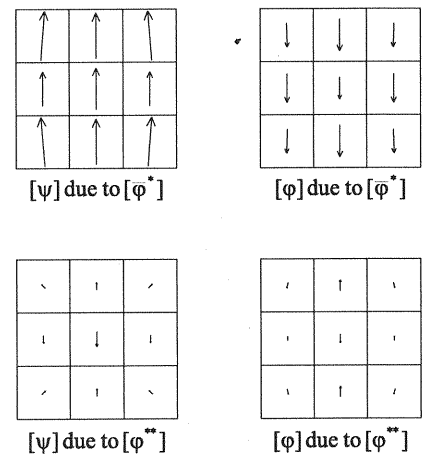

Fig. 5 Comparison of Fields due to Eigenvelocity with Actual Fields

rows, such that eigenvelocity vanishes there. As a more general setting, we use different $\boldsymbol{K}^o$ ($K_{22}^o = 5$) to make all elements have eigenvelocity. As shown in **Fig. 6**, eigenvelocities are distributed in all the elements, though there still exits $[\phi_P^{**}]$ which cannot be determined by solving Eq. (12). However, $\left[\overline{\phi}_P^*\right]$ determined from the boundary data produces almost the same pressure gradient and velocity fields in V^o, as in

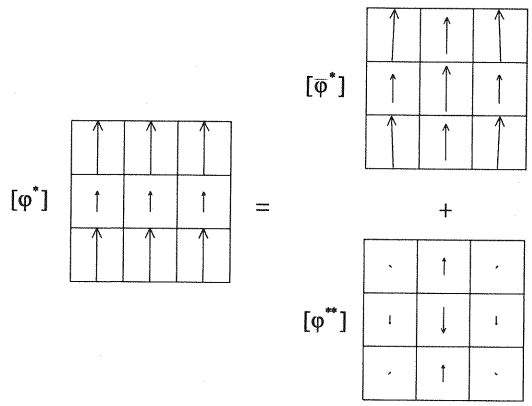

Fig. 6 Determined and Undetermined Eigenvelocity Components ($K^o_{22} = 5$)

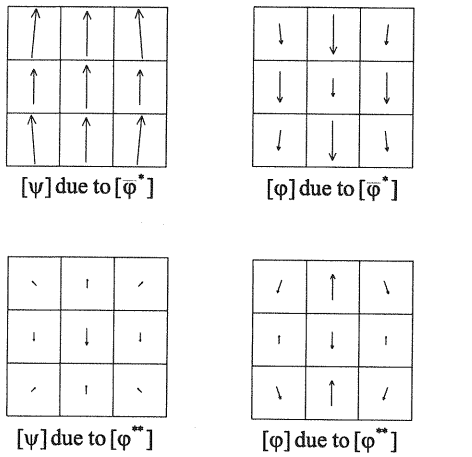

Fig. 7 Comparison of Fields due to Eigenvelocity with Actual Fields ($K^o_{22} = 5$)

the previous case; see **Fig. 7**. The field variables inside V can be estimated by using the data measured on the boundary, although the eigenvelocities which replace the heterogeneity are not fully identified.

Since $[\phi^{**}_P]$ is not known, we rewrite the second inverse problem, Eq. (13), assuming that $[\phi^{**}_p]$ corresponds to an eigenvelocity field $\boldsymbol{\phi}^{**}$ which satisfies $\int(g^{(1)} - g^{(2)})(\nabla \cdot \boldsymbol{\phi}^{**})\mathrm{d}V = 0$. The resulting inverse problem is expressed in the following discretized form for each element:

$$([K_{ab}] - [K^o_{ab}])\left[g^{(1)}_{aP}\right][\phi^{**}_P] + [K_{ab}][\psi_b] - [\phi^{**}_a] = [K^o_{ab}][\psi_b] + \left[\overline{\phi}^*_a\right], \tag{16}$$

where suffices a and b range from 1 to 2, but suffices P range from 1 to $2N^2 = 18$, and $\left[g^{(1)}_{aP}\right]$ yields a pressure gradient in the a-th direction of the element due to the P-th eigenvelicity. As is seen, Eq. (16) is

Table 2 Convergence of Eigenvelocities

element	comp.	initial	converged	exact
(1,1)	K_{11}	−1.076	−0.886	−1.
	K_{22}	−0.945	−0.971	−1.
	K_{12}	−0.023	−0.049	0.
(1,2)	K_{11}	−1.289	−0.671	−1.
	K_{22}	−1.350	−0.653	−1.
	K_{12}	−0.017	0.083	0.
(1,3)	K_{11}	−1.110	−0.925	−1.
	K_{22}	−0.962	−1.035	−1.
	K_{12}	−0.008	0.123	0.
(2,1)	K_{11}	−1.804	−1.299	−2.
	K_{22}	−1.793	−2.722	−2.
	K_{12}	−0.063	0.037	0.
(2,2)	K_{11}	−1.279	−197.1	−2.
	K_{22}	−1.035	−192.8	−2.
	K_{12}	−0.029	−180.8	0.
(2,3)	K_{11}	−1.804	−1.299	−2.
	K_{22}	−1.793	−2.722	−2.
	K_{12}	−0.063	0.037	0.
(3,1)	K_{11}	−1.110	−0.925	−1.
	K_{22}	−0.962	−1.035	−1.
	K_{12}	−0.008	0.123	0.
(3,2)	K_{11}	−1.289	−0.671	−1.
	K_{22}	−1.350	−0.653	−1.
	K_{12}	−0.017	0.083	0.
(3,3)	K_{11}	−1.076	−0.886	−1.
	K_{22}	−0.945	−0.971	−1.
	K_{12}	−0.023	0.049	0.

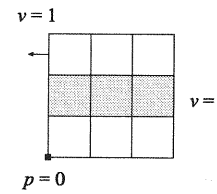

Fig. 8 Other Boundary Conditions Used in Inversion

no longer[8] linear with respect to unknown K_{ab} and ϕ^{**}_P. Applying the standard Newton-Raphson method to solve this non-linear equations with a condition of $[\Delta g_{AP}][\phi^{**}_P] = [0]$, we can obtain a converged solution. However, the resulting eigenvelocities nor permeability tensors are far from the exact solutions; see **Table 2** for the comparison of the initial and converged values of the eigenvelocities with the exact values in all nine elements. The prediction is not improved even if data of several boundary conditions are used as shown in **Fig. 8**.

The results obtained in the above analysis show the

[8] Since $\overline{\phi}^*$ produces the field variables which are almost the same as the exact ones, we may omit $\left[g^{(1)}_{aP}\right][\phi^{**}_P]$, to obtain an approximate linear equation.

limitation of identifying a material property distribution only by using data measured at the boundary. This is because the quantity of the data is insufficient as the rank of the square matrix is reduced, and a certain part of the eigenvelocity cannot be identified from the first inverse problem; this eigenvelocity corresponds[9] to $[\phi_P^{**}]$, which satisfies $[\Delta g_{IP}][\phi_P^{**}] = [0]$. While $[\phi_P^{**}]$ may not produce large flow, it is required to determine the final target, $[K_{ab}]$. Using data of different boundary conditions does not resolve this limitation. This is easily seen in the present formulation; only $\left[\Delta\phi_P^{(1)}\right]$ changes depending on the boundary conditions, and $[\Delta g_{IP}]$ remains the same as Green functions $g^{(1)}$ and $g^{(2)}$ are for fixed boundary conditions of zero pressure and zero flux. Hence, a common matrix $[\Delta g_{IP}]$ is used for other boundary data, and there are parts of eigenvelocity which corresponds to zero eigenvalue cannot be identified. This suggests that it is difficult to determine $[K_{ab}]$ in the second inverse problem, even when different boundary data are used.

4. EXAMPLE 2: PLASTIC PROPERTY IDENTIFICATION

The results of the preceding section show that the limitation of identifying material property distribution comes from the failure in solving the first inverse problem. In this section, we assume plane strain condition to more accurately identify the eigenfield, and then examine the limitation of solving the second inverse problem. To this end, we consider a case when V consists of an linearly elasto and ideally plastic material with unknown plastic property. The incremental behavior of V is determined by instantaneous elasto-plastic moduli which vary spatially and change as loading proceeds. The two inverse problems are for the eigenstress rate corresponding to plastic strain rate and the non-linear elasto-plastic constitutive relations. The strategy of the formulation remains the same, although the final form of the inverse problems will be slightly different from the previous one.

Let V be given as $\{(x_1, x_2, x_3)|(x_1, x_2) \text{ on } S\}$ with S being a traction-free boundary. This setting leads to the plane stress state in regions close to S. The displacement and traction on the boundary of S, denoted by ∂S, are measured. Furthermore, we assume that displacement data[10] on S, $(\overline{u}_1, \overline{u}_2)$, are available. They are denoted by $\overline{\boldsymbol{u}}(\boldsymbol{x}, \tau)$, with $\boldsymbol{x} = (x_1, x_2)$ and τ being a load parameter.

An associated flow rule is assumed, with an unknown yield function, $f(\boldsymbol{\sigma})$. This f determines instantaneous elasto-plastic moduli, $\boldsymbol{C}^{ep}$, as

$$\mathrm{d}\sigma_{ij} = C^{ep}_{ijkl}\mathrm{d}\epsilon_{kl} \tag{17}$$

where

$$C^{ep}_{ijkl} = \begin{cases} C_{ijkl} - \dfrac{(\boldsymbol{C}:\nabla f)_{ij}(\boldsymbol{C}:\nabla f)_{kl}}{\nabla f:\boldsymbol{C}:\nabla f} & f = 0 \text{ and } \mathrm{d}f = 0, \\ C_{ijkl} & f < 0 \text{ or } \mathrm{d}f < 0. \end{cases} \tag{18}$$

Here, $\boldsymbol{C}$ is a constant elasticity tensor and $(\nabla f)_{ij}$ stands for $\partial f/\partial\sigma_{ij}$. The governing equation for the displacement rate is now expressed in terms of $\boldsymbol{C}^{ep}$ as

$$\left(C^{ep}_{ijkl}(\boldsymbol{\sigma}(\boldsymbol{x}))\mathrm{d}u_{k,l}(\boldsymbol{x}, \tau)\right)_{,i} = 0, \tag{19}$$

where $\boldsymbol{\sigma}$ in the argument of $\boldsymbol{C}^{ep}$ emphasizes that $\boldsymbol{C}^{ep}$ changes depending on the stress state.

In order to formulate[11] the two inverse problems,, we replace the elasto-plastic constitutive relations, Eq. (17) and Eq. (18), in the form which is readily used in the equivalent inclusion method, i.e.,

$$\mathrm{d}\sigma_{ij} = C_{ijkl}(\mathrm{d}\epsilon_{kl} - \mathrm{d}\epsilon^p_{kl}), \tag{20}$$

where $\mathrm{d}\boldsymbol{\epsilon}^p$ is a plastic strain increment, defined as

$$\mathrm{d}\epsilon^p_{ij} = \begin{cases} \dfrac{\mathrm{d}\boldsymbol{\epsilon}:\boldsymbol{C}:(\nabla f)}{(\nabla f):\boldsymbol{C}:(\nabla f)}(\nabla f)_{ij} & f = 0 \text{ and } \mathrm{d}f = 0, \\ 0 & f < 0 \text{ or } \mathrm{d}f < 0. \end{cases} \tag{21}$$

If $-\boldsymbol{C} : \mathrm{d}\boldsymbol{\epsilon}^p$ is replaced by $\mathrm{d}\boldsymbol{\sigma}^*$ in Eq. (20), the governing equation of Eq. (19) becomes

$$C_{ijkl}\mathrm{d}u_{k,li}(\boldsymbol{x}) + \mathrm{d}\sigma^*_{ij,i}(\boldsymbol{x}) = 0. \tag{22}$$

The first inverse problem for $\mathrm{d}\boldsymbol{\sigma}^*$ can be formulated in the same manner as in Eq. (7), by using data on ∂S only. The identification of $\mathrm{d}\boldsymbol{\sigma}^*$, however, will be limited. When $\overline{\boldsymbol{u}}$ on S are available, we can determine $\mathrm{d}\boldsymbol{\sigma}^*$ more accurately; for instance, we determine $\mathrm{d}\sigma^*_{ij,i}$ using Eq. (22) and integrate to obtain $\mathrm{d}\boldsymbol{\sigma}^*$, or, decomposing $\mathrm{d}\boldsymbol{u} = \mathrm{d}\boldsymbol{u}^h + \mathrm{d}\boldsymbol{u}^d$ in the same manner as shown in Section 2, we have

$$\mathrm{d}u^d_i(\boldsymbol{x}; \mathrm{d}\boldsymbol{\sigma}^*) = \dot{\overline{u}}_i(\boldsymbol{x}, \tau)\mathrm{d}\tau - \mathrm{d}u^h_i(\boldsymbol{x}). \tag{23}$$

Recall that $\mathrm{d}\boldsymbol{u}^d$ is linear to $\mathrm{d}\boldsymbol{\sigma}^*$; see Appendix A. Once $\mathrm{d}\boldsymbol{\sigma}^*$ is determined, plastic strain rate and stress are determined as $\mathrm{d}\boldsymbol{\epsilon}^p = -\boldsymbol{C}^{-1} : \mathrm{d}\boldsymbol{\sigma}^*$ and $\boldsymbol{\sigma} = \boldsymbol{C} : \overline{\boldsymbol{\epsilon}} + \int \mathrm{d}\boldsymbol{\sigma}^*$. Hence, the second inverse problem is

$$\text{determine } f \text{ from relation between } \mathrm{d}\boldsymbol{\epsilon}^p \text{ and } \boldsymbol{\sigma}. \tag{24}$$

Note that the relation between $\mathrm{d}\boldsymbol{\epsilon}^p$ and $\boldsymbol{\sigma}$ should be checked point-wisely.

Assuming a von Mieses yield function, $f = J_2 - \sigma_y$ with J_2 being the second invariant of the deviatoric stress $(\sigma_{ij} - \delta_{ij}(\sigma_{pp}/3))$, and σ_y being unknown yield stress, we carry out a numerical simulation[12] of identifying this f. We consider a rectangular S subjected to concentrated forces; see **Fig. 9**.

[9] A vector $[\phi_a^{**}]$ includes a part of $\boldsymbol{\phi}^*$ which satisfies $\phi^*_{p,p} = 0$.

[10] Such a displacement field can be measured through the image analysis of the surface deformation[13]

[11] Unknown f can be determined by minimizing an error of a trial yield function. However, this is unrealistic, in particular when no information of f is available.

[12] The simulation $48 \times 42 \times 1$ three-dimensional eight-node-elements; the element is specially tuned for the elasto-plastic analysis as it is implemented with the Ruhnge-Kutta algorithm of up to the sixth order.

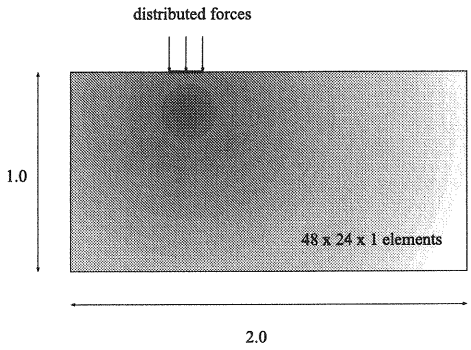

Fig. 9 Rectangular S

Since plastic strain increment does not have volumetric part ($\mathrm{d}\epsilon^p_{ii} = 0$), we solve Eq. (23) assuming $\mathrm{d}\sigma^*_{ii} = 0$. **Figure 10** shows the comparison of $\mathrm{d}\boldsymbol{\sigma}^*$ obtained from Eq. (23) with the exact value, $-\boldsymbol{C} : \mathrm{d}\boldsymbol{\epsilon}^p$. The distribution and the contour map of $\mathrm{d}\boldsymbol{\sigma}^*$ and $-\boldsymbol{C} : \mathrm{d}\boldsymbol{\epsilon}^p$ are plotted for small and large plastic deformations with the maximum shear strain being 0.0063 and 0.0374, respectively. As is seen, $\mathrm{d}\boldsymbol{\sigma}^*$ is in good agreement with the exact values. The distribution and the contour map of $\boldsymbol{\sigma}$ computed by using Eq. (24) is also plotted in **Fig. 11**. The exact distribution of $\boldsymbol{\sigma}$ is also shown in these figures for the comparison. The stress distribution obtained by the inversion coincides well with the exact stress distribution. Therefore, the form of f and the unknown σ_y can be determined by plotting $-\boldsymbol{C} : \mathrm{d}\boldsymbol{\sigma}^*$ in the principle stress space. **Figure 12** shows the principle plastic strain increment in the principle stress plane; a line corresponds to a plastic strain increment, $(\mathrm{d}\epsilon^p_1 - \mathrm{d}\epsilon^p_3, \mathrm{d}\epsilon^p_2 - \mathrm{d}\epsilon^p_3)$, starting from a point of $(\sigma_1 - \sigma_3, \sigma_2 - \sigma_3)$. In the exact solution, large plastic strain increments are initiated along an ellipse which corresponds to a yield surface. Due to errors in the inversion of the plastic strain increments and the stress state, a yield surface cannot be recognized as clearly as in the exact solution. However, the surface fairly tells the exact value of $\sigma_y = 0.001$.

As is seen, the first inverse problem can be solved accurately. An assumption[13] of $\mathrm{d}\sigma^*_{ii} = 0$ may play a key role; two components of $\mathrm{d}\sigma^*_{ij,i}$ are determined from Eq. (22), and hence the two independent components[14] of $\mathrm{d}\boldsymbol{\sigma}^*$ can be found by suitably integrating their gradients. The second inverse problem is also solved as accurately as the first problem. This is quite reasonable since solving the first problem is identical with determining field variables locally. While homogenous f of the simplest form is used, we can expect that the present formulation is applied even to heterogeneous elastic or more complicated plastic constitutive relations, if the deformation process is followed at each point and sufficient amount of local field variables are accumulated; for instance, heterogeneous elastic moduli can be readily determined when sufficient number of stress and strain (or their rate) are obtained by solving the first inverse problem. In the present formulation, the key in identifying the material property distribution is to solve the first problem as accurately as possible.

[13] Another condition can be used. Such a condition should be derived from assumptions which are physically acceptable.

[14] In numerical computation, it is easier to solve this equation than Eq. (23). The eigenstress rate can be obtained by applying the finite difference.

5. CONCLUDING REMARKS

The numerical simulation of the two illustrative problems shows the advantage of the formulation based on the equivalent inclusion method. It is easy to see quantities which can be determined from measured boundary data since a set of the formulated inverse problems are linear with respect to unknown functions. Therefore, the limit of identifying a material property distribution is clarified for a given measurement procedure or method. The following point should be emphasized: the present formulation yields a pair of linear inverse problems, and the analysis of the problems is easier than conventional problems due to the linearity.

As shown in Section 4, it is possible to identify inelastic material properties near a traction free surface, assuming the plane stress state. The specific form of, say, a yield function is not necessary as field variables such as stress and strain are first determined. We are applying the present formulation to various materials. For instance, shear bands in a material sample are one target. The deformation of regions surrounding the shear bands is measured by applying the image analysis. Inelastic heterogeneous properties as well as stress distribution of Japan island are another target. The GPS data are used to measure the surface deformation of Japan.

Appendix A EXPRESSION IN TERMS OF GREEN'S FUNCTIONS

Let $\boldsymbol{g}^{(1)} = \boldsymbol{g}^{(1)}(\boldsymbol{x}, \boldsymbol{y})$ be a Green function of V^o for zero displacement on ∂V. That is,

$$\begin{cases} C^o_{ijkl} g^{(1)}_{kp,li}(\boldsymbol{x}, \boldsymbol{y}) + \delta_{jp}(\boldsymbol{x} - \boldsymbol{y}) = 0 & \text{in } V^o, \\ g^{(1)}_{jp}(\boldsymbol{x}, \boldsymbol{y}) = 0 & \text{on } \partial V^o. \end{cases}$$

Suffices following the comma stands for the derivative with respect to $\boldsymbol{x}$'s coordinates. Since $\sigma^*_{ij,i}$ is regarded as distributed body forces, Eq. (6) is formally solved as

$$u^{(1)d}_i = \int_{V^o} g^{(1)}_{ip} \sigma^*_{qp,q} \, \mathrm{d}V.$$

Similar Green's function, $\boldsymbol{g}^{(2)}$, can be determined for zero traction on S and zero displacement on $\partial V - S$. Hence, Eq. (7) is more explicitly expressed as

$$\int_{V^o} (g^{(1)}_{ip} - g^{(2)}_{ip}) \sigma^*_{qp,q} \, \mathrm{d}V = -u^{(1)h}_i + u^{(2)h}_i.$$

The first inverse problem for the eigenfield is expressed more explicitly if suitable Green's functions

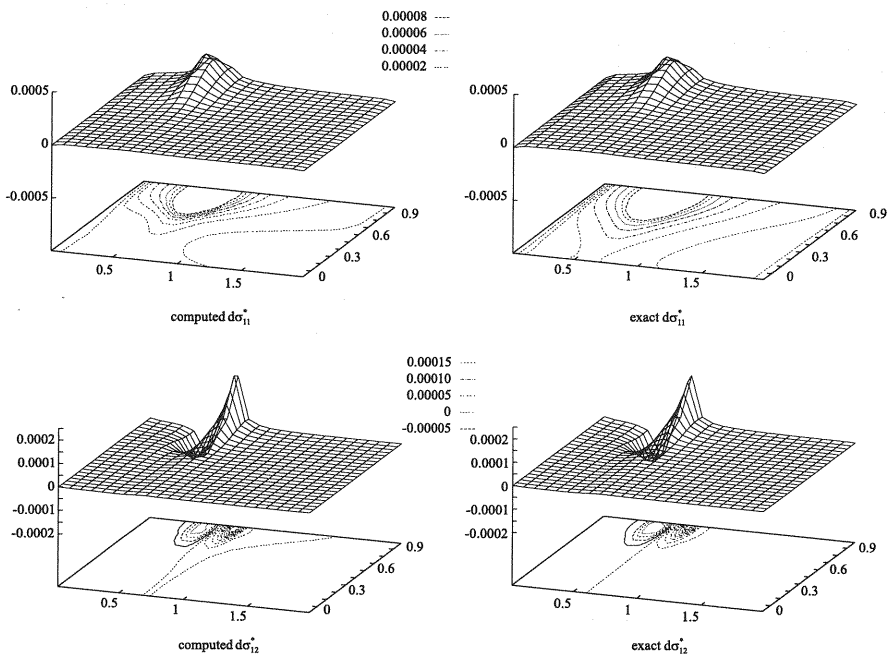

a) small plastic deformation

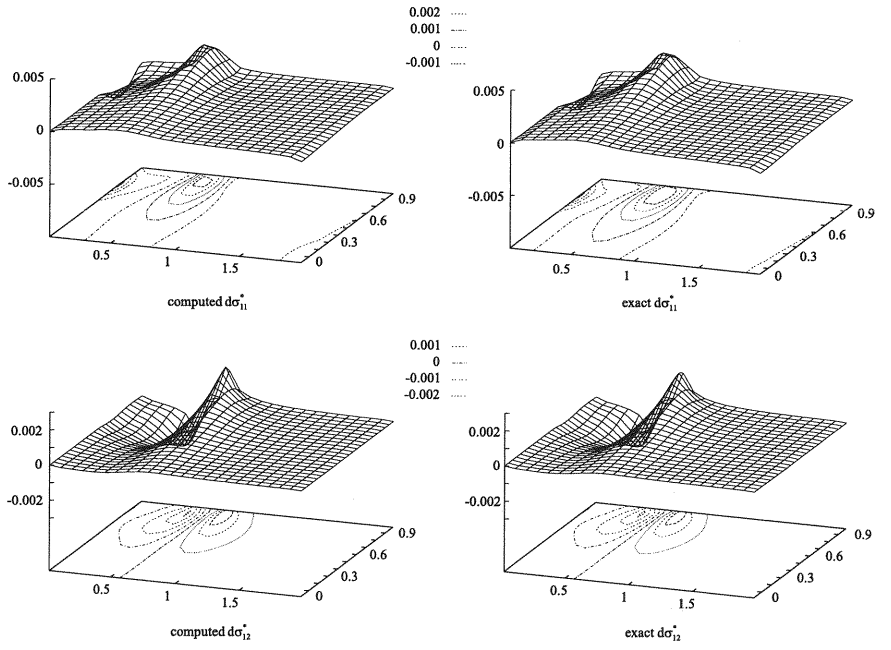

b) large plastic deformation

Fig. 10 Comparison of Computed Eigenstress Increment and Exact Values

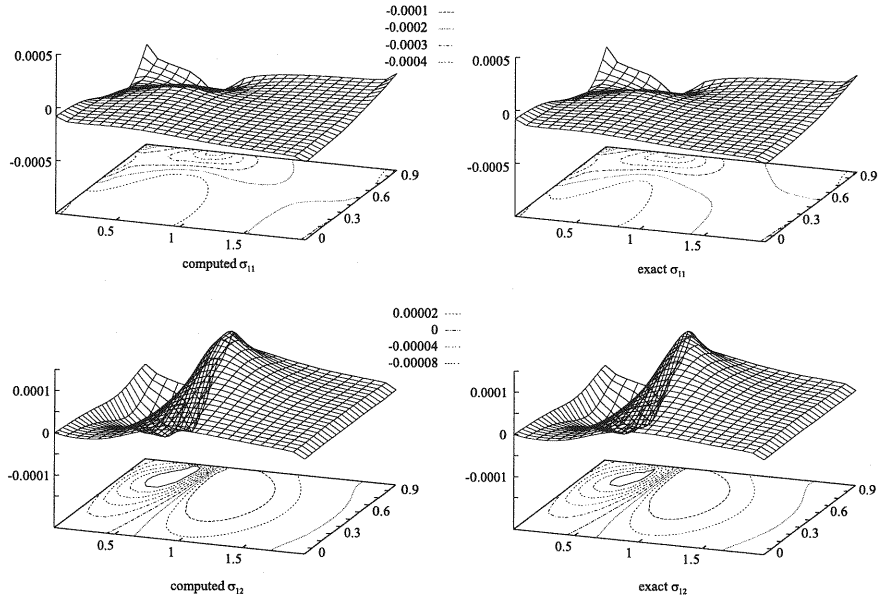

a) small plastic deformation

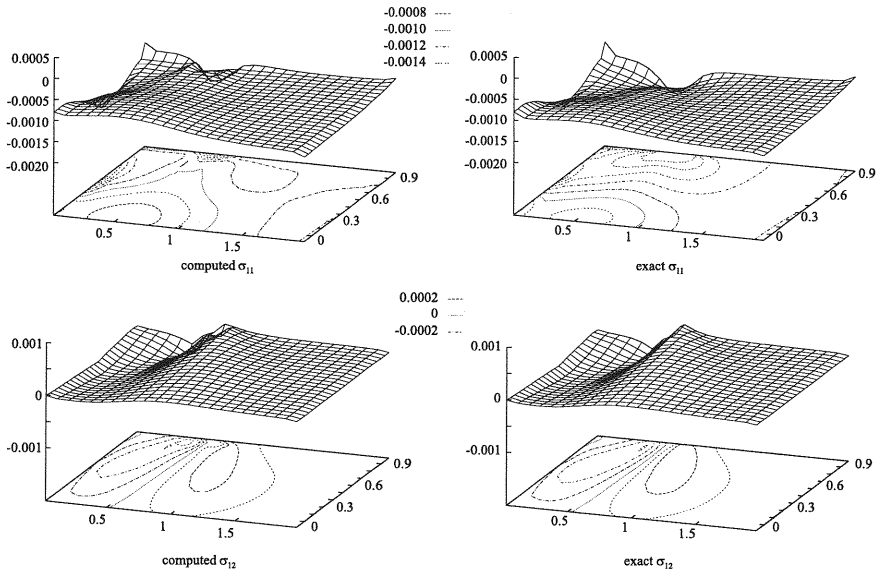

b) large plastic deformation

Fig. 11 Comparison of Computed Total Eigenstress and Exact Values

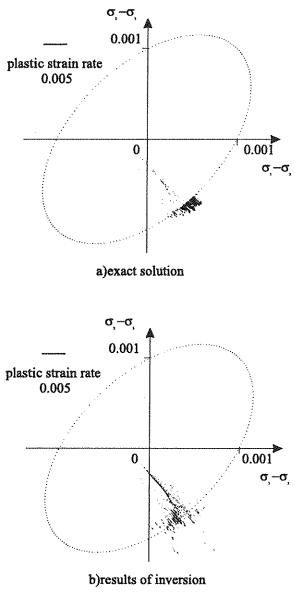

Fig. 12 Distribution of Plastic Strain

are used. For instance, denoting by $g^{(1)}$ and $g^{(2)}$ two Green's functions similar to $\boldsymbol{g}^{(1)}$ and $\boldsymbol{g}^{(2)}$ for the porous medium problem, we can rewrite Eq. (12)

$$\int_{V^o} (g^{(1)} - g^{(2)}) \phi^*_{q,q} \, \mathrm{d}V = -p^{(1)h} - p^{(2)h}.$$

Also, we can rewrite Eq. (23) as

$$\int_S g^{(1)}_{ip} \mathrm{d}\sigma^*_{qp,q} \, \mathrm{d}S = \dot{\bar{u}}_i - \dot{u}^{(1)h}_i.$$

Appendix B WEAK FORM OF BOUNDARY VALUE PROBLEM

Using a suitable virtual pressure, δp, we can obtain a weak form of Eq. (10), as

$$\int_{V^o} -\delta p_{,i} (K^o_{ij} p_{,j} + \phi^*_j) \, \mathrm{d}V + \int_{\partial V^o} \delta p n_i (K^o_{ij} p_{,j} + \phi^*_j) \, \mathrm{d}S = 0.$$

Hence, we can easily discretize this equation and apply the finite element analysis.

REFERENCES

1) Tanaka, M. and Bui, H.D. (eds.): *Inverse Problems in Engineering Mechanics*, Springer, 1992.
2) Bui, H.D.: *Inverse Problem in the mechanics of materials: An introduction*, CRC Press, New York, 1994.
3) Kubo, S.: *Inverse Analysis*, Baifu-kan, 1992 (in Japanese).
4) Murakami, A.: Application of Inverse Analyses to Engineering Problems, *Theoretical and Applied Mech.*, Vol. 46, pp. 25-37, 1997.
5) Nishimura, N.: Crack Determination Problem, *Theoretical and Applied Mech.*, Vol. 46, pp. 39-57, 1997.
6) Hirose, S.: Inverse scattering for flaw type classification, in *Inverse Problems in Engineering Mechanics*, Springer, New York, pp. 359-366, 1992.
7) Tosaka, N. and Utani, A.: Identification analysis of elastic constants using Kalman filter-boundary element method, *J. of Struct. Eng.*, AIJ, No. 446, pp. 41-50, 1993 (in Japanese).
8) Okuno, T., Suzuki, M. and Honjo, Y.: Optimum groundwater modeling and identification of hydraulic conductivities based on ABIC and extended Kalman fiter algorithm, *Proc. JSCE*, 1997 (in print).
9) Sakurai, H., S. Akutagawa, and O. Tokutome: Inverse Analysis of Inelastic Strain Based on Norm Minimization, *JSCE*, 517/III-31, pp. 69-74, 1996.
10) Eshelby, J.D.: *Proc. Roy. Soc.*, Vol. A241, pp. 376-396, 1957.
11) Nemat-Nasser, S. and M. Hori: *Micromechanics: Overall Properties of Heterogeneous Materials*, North-Holland, London, 1993.
12) Hori, M. and Hosokawa, N.: Inverse Analysis Based on Equivalent Inclusion Method, *Proc. of Struct. Eng.*, 1997 (in press).
13) Hori, M., H. Goto and. S. Adatchi: Accurate Image Analysis on Failure Process of Ground Mold Reinforced by Gotextile, in *Symposium on Inverse Analysis and Construction Control in Geoengineering*, 151-156, 1997 (in Japanese).

(Received June 15, 1998)